

Molecular adsorption and dissociative reaction of oxygen on the Si(111)7×7 surface

T. Hoshino

*Faculty of Pharmaceutical Sciences, Chiba University, 1-33 Yayoi-cho, Inage, Chiba 263-8522, Japan
and Texas Instruments Tsukuba Research and Development Center Limited, 17 Miyukigaoka, Tsukuba 305-0841, Japan*

Y. Nishioka

*Texas Instruments Tsukuba Research and Development Center Limited, 17 Miyukigaoka, Tsukuba 305-0841, Japan
(Received 17 June 1999)*

Reaction paths for the adsorption and dissociation of O₂ molecules on a Si(111)7×7 surface have been presented by theoretical computations. The adsorption of an O₂ molecule produces a molecular precursor, and the subsequent O₂ dissociation leads to a stable oxidized species. An attack of another O₂ molecule on the molecular precursor also gives stable states through the adsorption and dissociation process. In both reaction paths, small energy barriers appear before the O₂ molecular adsorption and the O₂ dissociation requires substantial activation energies of 1.3 eV. The electron distributions and density of states have been examined for several stable configurations along the reaction paths. The characteristic properties of these configurations are discussed and compared with experimental data.

I. INTRODUCTION

The initial stage of O₂ reaction with Si(111) surfaces has been extensively studied because of the significant importance of silicon oxide in applications for microelectronic materials. It has been accepted after many studies, over decades, that the adsorption of an O₂ molecule onto a Si(111)7×7 reconstructed surface presents a molecular precursor preceding the dissociative oxidation. In early studies,^{1,2} the O₂ molecular precursor was detected using spectroscopic techniques. A measurement of the work-function shift of the Si surface³ also suggested the presence of a molecular precursor after an O₂ gas exposure at very low temperatures. Recent detailed experiments using the photofragmentation technique⁴ or the optical second-harmonic generation method⁵ have clarified that this molecular precursor had a considerably long lifetime at room temperatures preceding the conversion into the stable dissociated state. However, the atomic configuration of the stable O₂ molecular precursor has not been identified yet. And the absence of a clear model for its atomic geometry still makes the existence of the O₂ precursor debatable.

An understanding of the oxidation reaction is indispensable for developing the technology for fine fabrication of silicon oxide films. In order to clarify the kinetics of the oxidation of a Si surface by O₂ molecules, several theoretical studies⁶⁻⁸ were performed for the Si(100)2×1 surface. In our previous work,⁷ an oxidation reaction was examined in which an O₂ molecule attacked a Si dimer by inserting one of the O atoms into the Si dimer bond. This O₂ dissociative reaction required a large activation energy. On the other hand, Kato, Uda, and Terakura⁸ found an alternative reaction path that required no activation energy when an O₂ molecule approached a Si(100) surface keeping its molecular axis parallel to the surface and interacting with two Si dimers simultaneously. Because of tight constraint on the orientation of the incident O₂ molecule, the channel of this reaction seemed to be narrow, as noted in their paper. But, this reaction path is expected to be possibly dominant at room, or lower, tem-

peratures. For the Si(111) surface, a reaction was investigated in which an O₂ molecule interacted with a single dangling bond on a Si surface and a dissociative oxidation occurred as a consequence of the interaction.⁹ However, there is no theoretical study for two O atoms of an O₂ molecule simultaneously interacting with a Si surface.

One of the most powerful experimental techniques to investigate the oxidation reaction of Si surfaces is the pulsed molecular-beam reactive scattering method.¹⁰ This method can provide some information on the activation process through the reaction of incident O₂ or O pulses with a Si surface by detecting the desorption of monoxide SiO species. In the literature,^{10,11} the O₂ reaction was first investigated on a Si(100) surface, but some reports^{12,13} suggested that no difference was detected in the reaction kinetics between Si(100) and Si(111) surfaces. Usually, the pulsed molecular-beam scattering analysis is performed at high temperatures, e.g., 850~950 °C.¹¹ Hence the Si(111) surface shows a disordered 1×1 structure in the experiments because the critical temperature for the 7×7 phase transition is about 830 °C.¹⁴ A recent theoretical work on the reaction of O₂ molecules or O atoms with Si(111)1×1 surfaces⁹ has successfully presented a reasonable interpretation of the kinetics of silicon oxidation and SiO desorption in experiments at high temperatures. This work with the 1×1 surface, however, was insufficient to interpret the experimental findings at room, or lower, temperatures. In the present paper, the investigation will be focused on the reaction of O₂ molecules with Si(111)7×7 surfaces by constructing a computational model representing a part of the 7×7 reconstructed structure. In particular, the interaction of an O₂ molecule with two dangling bonds will be closely examined. In spite of the highly restricted posture of the O₂ molecule, such a reaction path might have a dominant role at room, or lower, temperatures.

Many scanning tunneling microscope (STM) studies on O₂ adsorption on Si(111)7×7 surfaces¹⁵⁻¹⁷ met a consensus on the point that two types of oxygen-induced sites appeared at a very early stage after an exposure to O₂. One site was

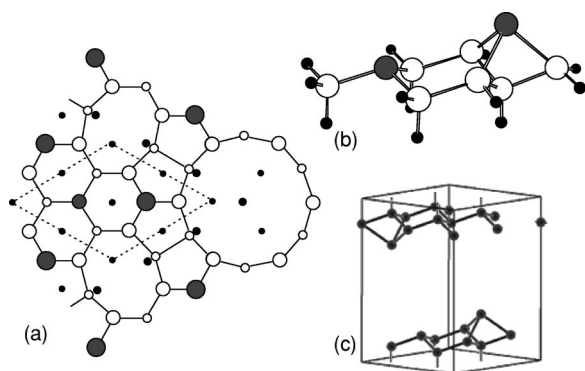


FIG. 1. (a) Top view of the corner region of the Si(111)7 \times 7 DAS structure. The large and small hatched circles denote the Si adatoms and the restatom. The open circles denote the atoms in the first bilayer, and the other atoms, in the underlayer, are represented by small dots. The 2 \times 2 area indicated by a dashed line is the focus in the present work. (b) Computational cluster model representing the 2 \times 2 area in (a). Small solid spheres denote the embedding H atoms. (c) Slab model representing the 2 \times 2 area in (a).

observed to be brighter and the other darker than the normal unreacted Si adatom sites. Further, the number of dark sites increased with the duration of O₂ exposure. One study¹⁸ tried to identify the bright and dark species employing detailed scanning tunneling spectroscopy (STS). Another study¹⁹ combining STM with ultraviolet photoelectron spectroscopy (UPS) provided valuable information. A theoretical investigation²⁰ was also performed to propose candidates for the species. In spite of these efforts, a clear assignment, or identification, of the bright and dark sites appearing in STM images has not been achieved yet. In this work, on the basis of computational results for the O₂ reaction, structures for the stable O₂ molecular precursor and the dissociative oxidation state on a Si(111)7 \times 7 surface are presented, and the consistency with experimental findings is discussed. Theoretical techniques of *ab initio* cluster calculations and first-principles band calculations have been adopted for this purpose. Cluster calculations provide molecular orbitals (MO's) whose electron density distribution are reflected in STM images, and band calculations with the supercell method provide the density of states (DOS) which enable a comparison with spectrums from UPS and STS experiments to be made.

II. METHOD OF CALCULATION

A schematic illustration of a part of the dimer–adatom–stacking-fault (DAS) structure for the Si(111)7 \times 7 reconstruction is shown in Fig. 1(a). The large and small hatched circles denote the Si adatoms and the restatom, respectively, all of which have a surface dangling bond. A single corner hole and two dimer rows are depicted in (a). The present research focuses on the 2 \times 2 area indicated by a dashed line which contains an adatom and restatom pair on the 7 \times 7 surface. Both a cluster and a slab model were constructed to represent the surface structure of this 2 \times 2 area. The cluster model shown in (b) was employed for MO calculations to determine the lowest potential-energy reaction paths. This model contains the adatom, the restatom, and the atoms in the first bilayer. The lower and outer part of this cluster is

embedded between 12 H atoms. During geometry optimization, all Si atoms are allowed to move within the constraint of the Cs symmetry whereas the H atoms were fixed to maintain a crystalline structure. The slab model in (c) was employed for the band calculation to compute the DOS using the stable atomic configurations obtained by the cluster calculation. The model consists of a supercell with a slab structure containing a vacuum spacing of 8.6 Å. Periodic boundary conditions are applied in all directions. The slab contains the adatom, the restatom, and the atoms in the first bilayer, plus their inversions. The unit-cell dimensions are 7.68 \times 7.68 \times 12.52 Å.

The reaction paths were determined through the geometry optimization to find the stable and saddle points on the potential energy hypersurface, using the *ab initio* unrestricted Hartree-Fock (HF) MO method.²¹ The intrinsic reaction coordinates (IRC) were obtained along the steepest descending gradient from the saddle point to the stable point for both directions of the reactant and product. The potential-energy change along the reaction path was estimated by the second-order Møller-Plesset perturbation theory (MP-2),²¹ in which the HF level computation was improved by taking electron correlation into account. The basis function was a split-valence-type basis set, 3-21G*.²² Band calculations with the slab model were performed with the local-density approximation in the Vosko-Wilk-Nusair (VWN)-type formalism²³ for the exchange-correlation energy, using norm-conserving pseudopotentials²⁴ and a plane-wave basis set with an energy cutoff of 40 Ry. The DOS was computed using eight *k* points in the Brillouin-zone sampling.

III. RESULTS

A. Reaction of an O₂ molecule with the Si(111)7 \times 7 surface

Figure 2 shows the atomic configurations and the potential-energy change during the adsorption of an O₂ molecule on the Si(111)7 \times 7 surface. The zero level of this potential energy curve corresponds to an infinite separation of the O₂ molecule from the Si surface. Since the ground electronic state of an isolated O₂ molecule is the spin triplet, computations have been performed with the spin triplet state assuming the spin electronic state of the Si surface is the singlet. Initially the O₂ molecule weakly adheres to the Si surface with a very slight energetic stabilization of 0.2 eV as indicated by the shallow minimum. The O-O bond length hardly changes from that of the isolated O₂ molecule (1.24 Å). There exists a potential-energy barrier for this O₂ adsorption reaction. In the transition state, the O-O bond length expands to 1.31 Å, and each O atom starts to make a chemical bond with the Si adatom or restatom. The energy at the transition state is 0.8 eV, which is the activation energy required for the adsorption reaction of the O₂ molecule. Beyond the transition state, the potential energy decreases steadily and an O₂-adsorbed structure with an Si-O-O-Si configuration is generated. The reaction product is depicted as the O₂ adsorption state. The stabilization energy of this reaction is 4.2 eV.

The lowest energy path for the subsequent dissociative reaction is shown in Fig. 3. The potential-energy curve is presented relative to the initial O₂ infinite separation. Computations were performed with the spin triplet state. There

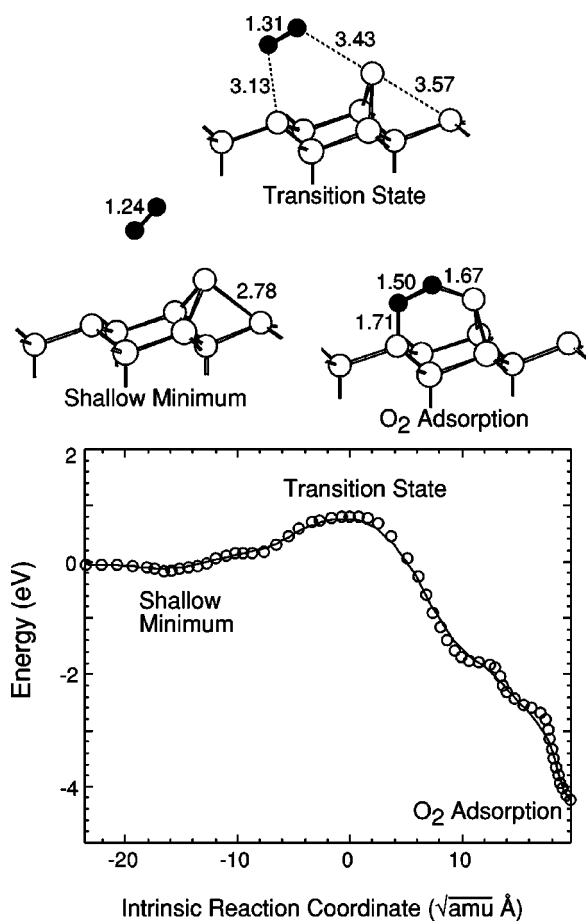


FIG. 2. Potential-energy curve for the O_2 adsorption on the Si(111) 7×7 surface. The abscissa represents the distance from the transition state measured in the mass-weighted Cartesian coordinates. Atomic configurations for the shallow minimum, the transition state, and the O_2 adsorption are exhibited with bond lengths in units of Å. H atoms are not shown for the sake of visual clarity. Open and filled spheres denote Si and O atoms, respectively.

appears two potential energy barriers through this path. The atomic configuration of the first transition state suggests the dissociation of the O_2 molecule. Although the O-O bond length does not expand compared with the preceding O_2 adsorption structure, the potential energy increases by 1.3 eV. Passing over the first transition state, a stable configuration is generated by the separation of the O-O pair. In this stable structure, each of two O atoms is strongly bound to the Si adatom or the restatom. In particular, the chemical bonds are saturated around the Si adatom in a carbonyl-like configuration with an Si-O double bond. A small energetic activation of 0.6 eV is required to overcome the potential barrier of the second transition state. This second transition state is responsible for the formation of a chemical bond between the Si adatom and the O atom bound to the Si restatom. It is suggested from the potential-energy curve that the reversed reaction involving the second transition state is unfavorable, that is, the formation of the Si-O bond easily occurs in spite of the difficulty of the Si-O dissociation. Finally an O_2 -dissociated structure with an Si-O-Si-O configuration is generated. This final reaction product is depicted as the dissociative oxidation state, and its generation releases a stabilization energy of 3.0 eV measured from the O_2 adsorption structure.

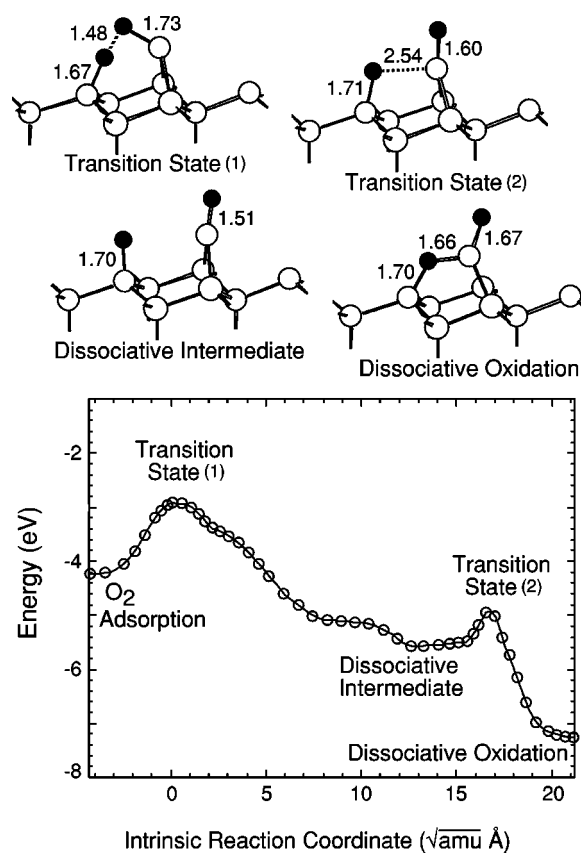


FIG. 3. Potential-energy curve for the subsequent oxidation of the Si surface. The abscissa represents the distance measured from the first transition state. Atomic configurations for the first transition, the intermediate, the second transition, and the dissociative oxidation states are exhibited. See also the legend of Fig. 2.

B. Reaction of another O_2 molecule with the O_2 -adsorbed surface

Figure 4 shows the potential-energy change and the atomic configurations where another O_2 molecule attacks the O_2 adsorption state of Fig. 2. The potential energy is presented relative to an O_2 infinite separation. The computation was started with the O_2 -adsorbed Si surface and the additional O_2 molecule, both of which contained two unpaired electrons, so that each part represented the spin triplet state. Initially an additional O_2 molecule weakly adheres to the Si adatom with a slight expansion of the O-O bond. Beyond the small potential-energy barrier (0.1 eV), the O_2 molecule attaches to the Si adatom in an Si-O-O configuration. This O_2 adsorption gives an energetic stabilization of 2.8 eV, and the configuration is designated as intermediate. In the subsequent dissociative reaction, the potential energy rapidly increases with the O-O separation. The atomic configuration of the transition state suggests the dissociation of the O_2 molecule, and the potential energy barrier measured from the preceding intermediate state is 1.3 eV. The reaction proceeds to generate a very stable configuration with the formation of a bond between the dissociated O atom and the first-layer Si atom. A configuration of two Si-O bonds is produced in the O_2 dissociation state and the surface is fully terminated by O atoms. This O_2 dissociation reaction is also exothermic, releasing an energy of 2.1 eV measured from the intermediate state.

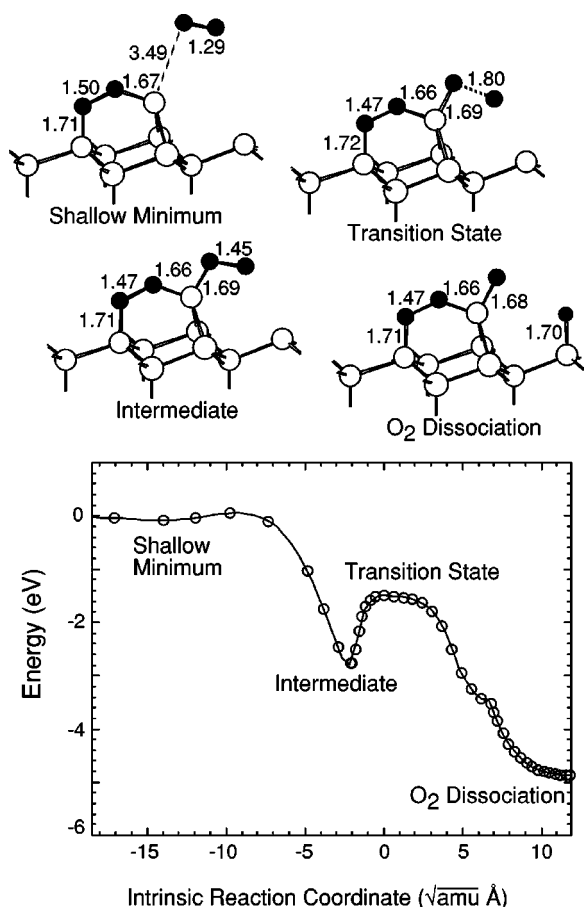


FIG. 4. Potential-energy curve for the attack of another O₂ molecule on the O₂-adsorbed Si surface. Atomic configurations for the shallow minimum, the intermediate, the transition, and the O₂ dissociation states are exhibited. See also the legend of Fig. 2.

C. Major stable structures

Several stable states appear along the reaction paths for the O₂ adsorption and the dissociative oxidation process in Figs. 2–4. The configurations and electron populations for the five stable states are shown in Fig. 5. It has been confirmed from supplementary computations that all those stable structures are obtained even in an optimization without the constraint of the Cs symmetry. In the clean surface state (a), the Si adatom resides on a T_4 site terminating with three surface dangling bonds. In the O₂ adsorption state (b), the O₂ adhesion dissociates one of the back bonds of the adatom and results in the Si-O-O-Si formation. The Si adatom is displaced toward the Si restatom. Since the O-O bond length in the transition state for the dissociative reaction was 1.7 Å in previous studies,^{7,9} the O₂ adsorption structure apparently maintains the O-O bond. The vertical height of the Si adatom increases, compared to its height at the T_4 site. In the dissociative oxidation state (c), a bridging formation is generated and the Si-O bond lengths and the Si-O-Si bond angle are close to the values of crystalline SiO₂. The Si adatom has a fourfold coordinate saturated by the dissociated O atom, making the Si-O-Si-O formation. In the intermediate state (d), another O₂ molecule is attached to the Si adatom while maintaining the O-O bond. The atom positions of the Si-O-O-Si scarcely vary from those of (b). In the O₂ dissociation state (e), the Si atom disconnected from the adatom is also

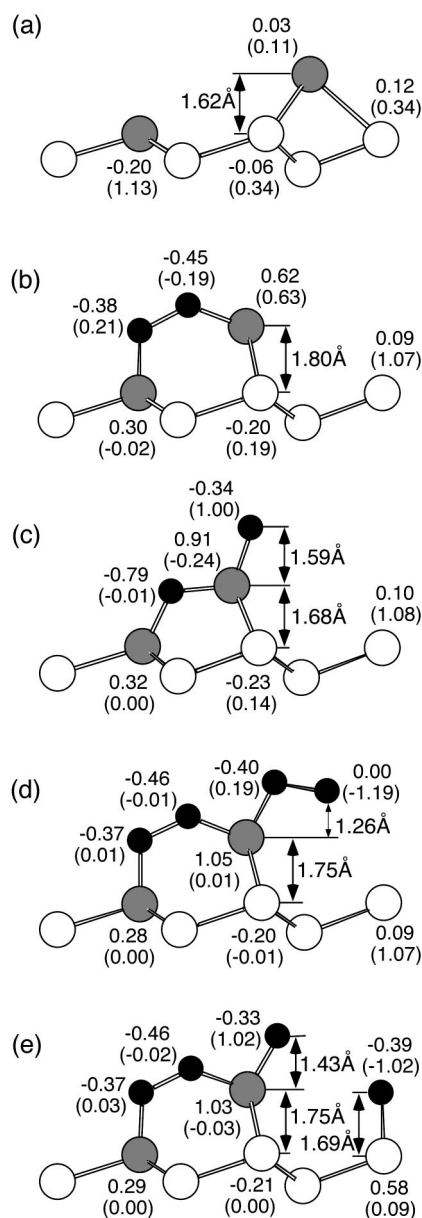


FIG. 5. Side views of the stable structures for (a) the clean surface, (b) the O₂ adsorption, (c) the dissociative oxidation, (d) the intermediate, and (e) the O₂ dissociation states. The solid spheres denote O atoms and the notation for the Si atoms is the same as in Fig. 1. Electron densities and α -spin densities are exhibited together with the vertical heights of the adatoms in units of Å.

saturated by the dissociated O atom. The restatom hardly shifts from the initial crystalline position during the reactions.

It is informative to examine the changes of the charge and spin distributions. Figure 5 presents the charge and α -spin (in parentheses) densities obtained by a Mulliken population analysis. In the clean surface structure (a), one of the unpaired electrons is localized on the Si restatom, and the other is distributed over the T_4 site around the Si adatom. In the O₂ adsorption structure (b), a charge transfer of $0.8e$ occurs between the Si atoms and the O₂ molecule. Due to this large charge transfer, the Si adatom and restatom become positive. In particular, the Si adatom is strongly positively charged, which induces the negative charging of the underlying Si

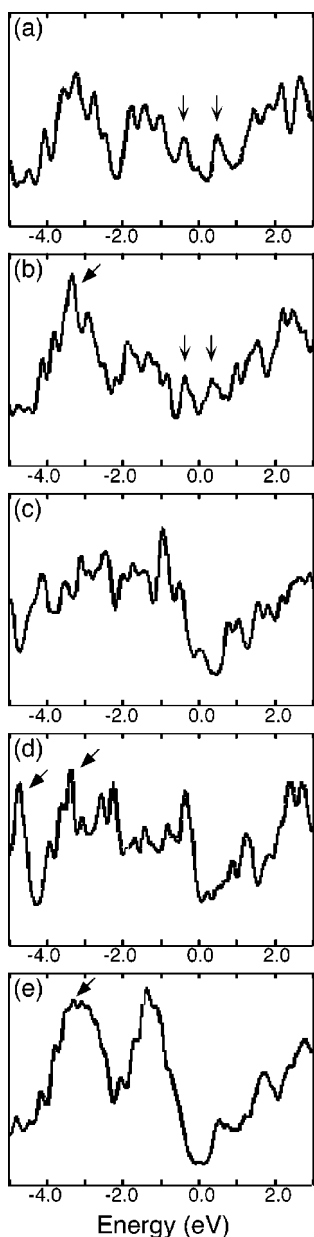


FIG. 6. Density of states for the stable structures in Fig. 5. The lines are presented in arbitrary units, and the Fermi energy level is set at zero.

atoms connecting to this adatom. Most of the α -spin density is localized on the Si adatom and the first-layer Si atom disconnected from this adatom. In the dissociative oxidation structure (c), a large electron transfer of $-0.8e$ occurs to the bridging O atom, whereas the electron transfer to the other O atom is moderate ($-0.3e$). These electron transfers make the Si adatom further positively charged. Two unpaired electrons are localized on the O atom attached to the top of the adatom and the Si atom disconnected from the adatom. In the intermediate structure (d), an electron transfer of $-0.4e$ occurs from the Si adatom to the newly bonded O atom in addition to the charge distribution of (b). Since the attaching O_2 molecule originally has two unpaired β electrons, the α -spin density at the adatom is canceled by the β -spin density. In the O_2 dissociation structure (e), an electron transfer of $-0.4e$ also occurs between the dissociated O atom and the

TABLE I. Electric dipole moment in the surface normal direction for the stable structures.

State	Dipole moment (Debye)
(a) clean surface	-0.72
(b) O_2 adsorption	1.48
(c) dissociative oxidation	1.20
(d) intermediate	3.16
(e) O_2 dissociation	4.51

Si atom disconnected from the adatom. Two unpaired electrons, one α and one β , are localized on the dissociated O atoms.

Figure 6 shows the calculated DOS curves of (a) the clean surface, (b) the O_2 adsorption, (c) the dissociative oxidation, (d) the intermediate, and (e) the O_2 dissociation structures. The striking feature of these curves is that the O_2 adsorption induces an appearance of a sharp peak at -3.3 eV; however, the peak disappears in the subsequent dissociation. The sharp peak at -3.3 eV is observed for (b), (d), and (e) and hence is considered to originate in the O-O bond in the Si-O-O-Si formation. Further, an additional sharp peak is seen in (d) at -4.7 eV. Another important feature in the curves of Fig. 6 is seen in changes of the DOS curves around the Fermi level. In (a), two distinct levels for the occupied and unoccupied states are present near the Fermi level with a band gap between them. In (b), there also exist two levels for the occupied and unoccupied states. On the other hand, the structure (c) has no significant states near the Fermi level and only shows a wide band gap. Neither are distinct levels observed in (d) and (e), and the band gaps are seen to be wider.

It is interesting to examine how the electric dipole moment changes throughout the reactions. Table I shows the dipole moment in the surface normal direction (outward pointing surface dipole) for the respective stable structures. In (a), the dipole moment has a negative value, which is easily understood from the fact that Si adatoms are positively charged on the clean surface.²⁵ In contrast, an adhesion of an O_2 molecule makes the dipole moment positive in (b) and (c). Further, another O_2 adhesion remarkably increases the value in (d) and (e). It should be noted that the O_2 adsorption state (b) has a larger electric dipole moment than the subsequent dissociative oxidation state (c).

IV. DISCUSSION

A. Initial stage of O_2 reaction with Si(111) surfaces

The present calculation has clarified that there appears an O_2 molecular precursor preceding the dissociative species in both the reactions caused by the first and second O_2 attacks on the Si surface. Slight activation energies are necessary for the adhesion of O_2 molecules to generate such molecular precursors. The potential-energy barrier for the conversion from the molecular precursor to the dissociative species is not small, 1.3 eV in both cases. Therefore it is natural to expect that an O_2 molecular precursor would be detected in experiments. Since both the adatom and the restatom contribute to the O_2 -adsorbed formation in the first O_2 attack, the presence of an adatom and restatom pair would be favorable

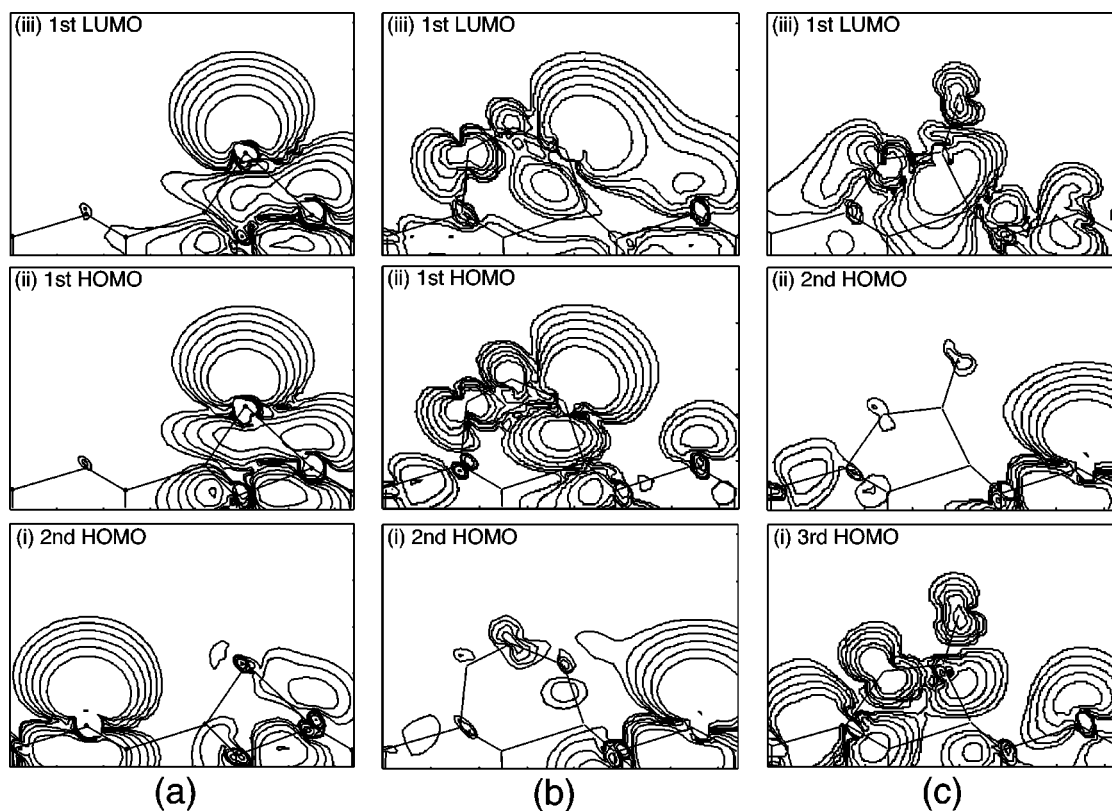


FIG. 7. Contour plots of electron density distributions in the frontier MO's of the stable structures of (a) the clean surface, (b) the O_2 adsorption, and (c) the dissociative oxidation state. The levels of the contour lines are 0.0001, 0.0002, 0.0004, 0.0008, 0.0016, and $0.0032e/\text{Bohr}^3$.

for the initial O_2 adsorption on the Si(111) surface. From this viewpoint, the 7×7 structure is considered to be very advantageous for the generation of molecular precursor states. In our previous studies,^{7,9} the activation energy required for the O_2 dissociative reaction was estimated to be 2.5~2.6 eV when an O_2 molecule reacts with a Si(100) 2×1 surface while maintaining its molecular axis perpendicular to the surface⁷ or reacts with a single dangling bond on a Si(111) 1×1 surface.⁹ Hence the value of the activation energy has been reduced by half. This would be due to the difference that each O atom of the incident O_2 molecule interacts with Si atoms on the surface in the present reactions whereas only one of the O atoms interacts with Si atoms in the previous cases.

The Si adatom has been allowed to move in the present geometry optimizations, which results in the dissociation of one of the back bonds of the adatom in the O_2 adsorption structure (b). Further, the adatom no longer resides on the initial T_4 site in the dissociative oxidation structure (c). This result means that the binding of adatoms on the T_4 site is not so tight, which is compatible with the following STM findings. In observations of 9×9 , 11×11 , and 13×13 DAS structures at 470 °C on Si(111) surfaces,²⁶ several interior adatoms escaped from the DAS reconstructed region and returned back again without breaking the framework of the $(2n+1) \times (2n+1)$ structures. $c2 \times 2$, $c2 \times 4$, or $c2 \times 8$ periodic structures were usually observed at room temperatures in those areas not occupied by the 7×7 DAS domains; however, these metastable structures could not be observed

above 400 °C,²⁷ and the areas showed disordered images due to the thermally excited random motion of the adatoms.

B. Electron distributions in frontier orbitals

Several STM observations to investigate the initial O_2 reactions on Si(111) 7×7 surfaces have given the same result; that is, an O_2 exposure initially generated bright spots at the sites where Si adatoms used to be imaged, and the sites turned dark with further O_2 exposure. Some researchers^{16,17} assigned both bright and dark sites to the dissociative states of O_2 . Another study¹⁹ reported that the bright site was essentially an O_2 molecular state, whereas the dark site was O atom-reacted state.

In this work, we have presented a reaction pathway for the O_2 adsorption and the subsequent dissociative reaction. It is interesting to extract the information concerning STM images from the data of the present theoretical calculations. Hence electron distributions have been surveyed for the occupied and the unoccupied MO's existing close to the Fermi level. Our previous studies on the clean and alkali metal-adsorbed Si(100) structures^{28,29} demonstrated that electron distributions in the frontier MO's reproduced experimental STM images well. Figure 7 shows electron distributions in some occupied and unoccupied MO's in the vertical plane that contains both the Si adatom and restatom. In the clean surface structure (a), most of the electron density in the second highest occupied MO (HOMO) resides around the restatom. On the other hand, electrons are localized on the adatom site in both the first HOMO and the first lowest un-

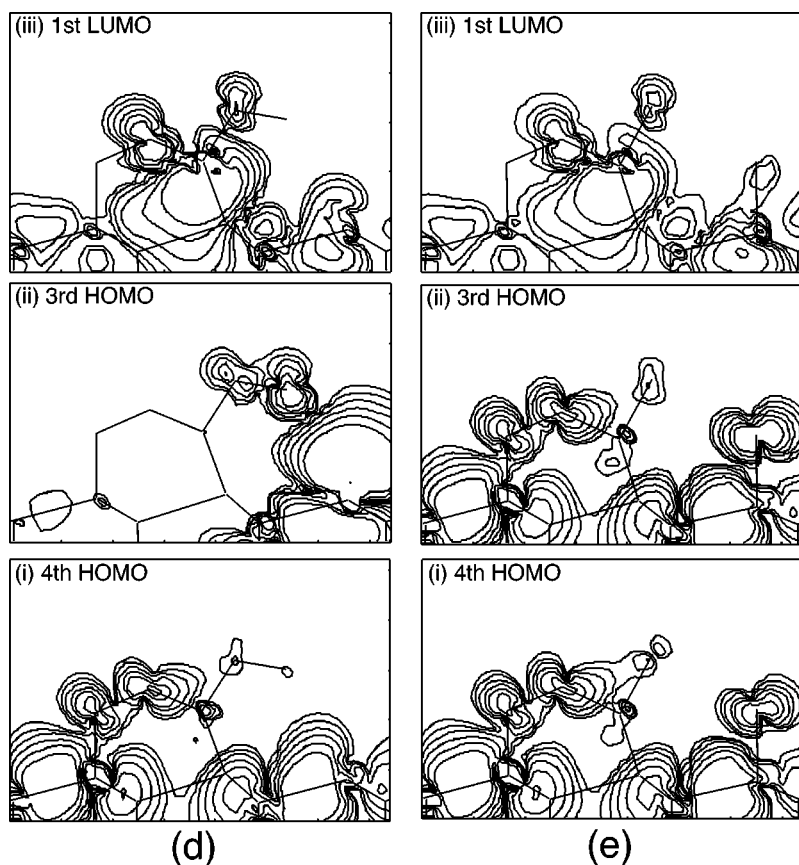


FIG. 8. Contour plots of electron density distributions in the frontier MO's of the stable structures of (d) the intermediate and (e) O_2 dissociation state. See also the legend of Fig. 7.

occupied MO (LUMO). These electron distributions, protruding upward from the surface, produce substantial signals in the STM images, which explains the basic STM results that Si adatoms are imaged brightly in both conditions of $(-)$ (filled state) and $(+)$ (empty state) sample biases. The most important feature in the O_2 adsorption structure (b) is that a large electron density is present at the adatom in the first HOMO and its distribution protrudes upward above the adatom. Further, the energy level of the first HOMO is shallower than that for the clean surface structure. A similar situation occurs in the unoccupied state, also. The first LUMO has a large electron distribution above the adatom and, further, the energy level is lower than that of the clean surface structure. Therefore it is concluded that this O_2 adsorption structure is imaged brightly in the STM observations in both the filled and empty states. Moreover, the brightness is expected to be larger than that for the normal Si adatom. It should also be noted that the electron distribution in the second HOMO is localized on the Si atom disconnected from the adatom. In the dissociative oxidation structure (c), the first HOMO represents a bonding between the adatom and the Si atoms in the underlayer, but no electron density is seen in the plane containing the Si adatom and restatom because the electron distribution has a node on the plane. The electron distribution of the second HOMO is similar to that of the second HOMO of (b); that is, electrons are localized on the Si atom disconnected from the adatom. Both the third HOMO and the first LUMO represent some bonding or antibonding characters of Si-Si or Si-O and give no significant contributions to STM images. The energy levels of these HOMO's and LUMO are deeper (HOMO's) or

higher (LUMO) than those of structures (a) and (b). Therefore the dissociative oxidation structure is concluded to be imaged remarkably darker.

Figure 8 shows electron distributions for the stable states generated by the attack of the second O_2 molecule. In the intermediate structure (d), the electron distributions of the first and second HOMO's have a node on the vertical plane, and no electron densities are seen in the view. In the third HOMO, electrons are localized on the Si atom disconnected from the adatom. Both the fourth HOMO and the first LUMO represent bonding and antibonding characters of Si-Si or Si-O and seem to give no contributions to STM images. The energy level of the third HOMO is close to that of the second HOMO of (c). Hence the intermediate structure would give a dark image comparable to structure (c). In the O_2 dissociation state (e), electron distributions of the third HOMO, fourth HOMO, and first LUMO represent bonding or antibonding characters with no protruding distributions. The energy levels of these HOMO's are the deepest among those of (a)–(e). Accordingly, the O_2 dissociation structure is concluded to be most darkly imaged in the STM observations.

Judging from the above results, the O_2 adsorption structure (b) seems to be one of the probable candidates for the molecular precursor that is brightly imaged in STM observations.

C. Molecular precursor and its spectroscopic properties

In addition to STM observations, spectroscopic experiments also provide important information for identifying the species on O_2 -reacted Si surfaces. A sharp peak at

-3.3 eV appeared in the calculated DOS curves in Fig. 6. In spite of the deviation of the peak position, this feature fairly agrees with the combined STM and UPS analysis by Dujardin *et al.*¹⁹ They indicated the appearance of a peak at 3.8 eV in the binding energy of the UPS spectrum upon an O_2 exposure. The intensity of the 3.8 eV peak increased with the number of bright sites in the STM images, and it decreased when the bright sites turned dark, which was their grounds for the assignment of the bright site to the O_2 molecular precursor.

The UPS experiment by Comtet *et al.*³⁰ suggested that the lifetime of the O_2 molecular precursor was considerably longer in ultrahigh vacuum conditions. They also showed a peak of 5.1 eV in addition to that of 3.8 eV and assigned both of them to O_2 molecular chemisorption. Namely, two types of long-lived molecular species were detected. The DOS curve (d) in Fig. 6 is compatible with their experiments, in which a sharp peak of -4.7 eV appears when an additional O_2 molecule is attached to the surface. The intermediate structure (d) has two O_2 molecules, and its DOS curve shows two sharp peaks. Therefore the second O_2 molecule, which makes a single bond with the Si surface, would be the origin of the peak of -4.7 eV.

STS data were sampled for various sites on the O_2 -exposed Si(111) surfaces by Avouris and Lyo.¹⁸ In their STS spectra (Fig. 4 in Ref. 18), adatoms are characterized by occupied and unoccupied states at ~ 0.3 eV below and above the Fermi level, bright sites have a spectrum that looks very much like that of an adatom but more intense, and dark sites show the absence of surface states. The calculated DOS curves are compatible with the STS data. In the clean surface structure (a), energy levels exist both below and above the Fermi level. These energy levels near the Fermi level are also present in the O_2 adsorption structure (b). On the other hand, the dissociative oxidation (c), intermediate (d), and O_2 dissociation (e) structures have no levels in the low binding-energy range.

Another STM work reported on the reactivity of the bright sites.³¹ Bright sites (named B sites in Ref. 31) were dominant reaction products after an exposure of a clean Si surface to O_2 . An additional O_2 exposure turned some B sites into dark sites (named D sites). Subsequently, these D sites were possibly transformed into original B sites by electron irradiation. Our theoretical results give a satisfactory explanation for this experiment by supposing that the B site is structure (b) and the D site is (d). Electron irradiation would detach the O_2 molecule from the intermediate state.

It would be reasonable to consider that there exist several possibilities for the configuration to generate bright or dark sites in STM images. Therefore the structures presented in this work should be regarded as one possible example for the species detectable in experiments.

D. Comparison with other experimental and theoretical work

An electron transfer of $-0.8e$ from the Si atoms to the O atoms ($-0.45e$ and $-0.38e$ in each O atom) occurs in the Si-O-O-Si formation of the O_2 adsorption structure (b). This result is consistent with experimental estimations with electron energy loss spectroscopy (EELS).³²

The necessity of the presence of adatom and restatom in pairs suggests that the number of O_2 molecular species, which are imaged brightly, cannot exceed 3 in a half unit cell of the 7×7 structure. This is compatible with the experimental findings that the ratio of bright sites to total Si adatoms saturates during an exposure of O_2 molecules.¹⁹

Measurement of the work function of a Si surface during exposure to O_2 suggested the presence of an O_2 precursor state preceding dissociative chemisorption.³ An O_2 exposure induced a large positive work function shift compared to the clean surface, and the amount of the shift was reduced by the conversion to a stable dissociative state. The change of the surface dipole moment obtained for structures (a), (b), and (c) in Table I is consistent with the feature of the above work function shift.

In the extended Hückel tight-binding calculations by Schubert, Avouris, and Hoffmann,²⁰ a variety of structures was discussed for assignment of the oxygen associated species on Si(111) surfaces. The O_2 adsorption structure (b) is close to the bridge configuration in their work. A major difference of (b) from their configuration is that the back-bond dissociation of the adatom enables a natural Si-O-O-Si formation.

Some configurations were assigned as candidates for the bright and dark site STM images in previous studies.^{16,20} In these reports, the bright sites were asserted to be caused by a configuration with an insertion of an O atom in the back bond of the adatom leaving the dangling bond intact, whereas the dark image was asserted to originate in a saturation of the adatom dangling bond with another O atom. The structures presented in this work agree with these ideas in the sense that the activation and inactivation of the dangling bond at the adatom are responsible for the bright and dark site images.

Site hopping of a molecular O_2 species on Si(111) 7×7 surfaces was observed in an STM experiment by Hwang, Lo, and Tsong.³³ The hopping mainly occurred between adjacent adatom sites in a 7×7 half unit cell. In Fig. 3, we have examined the reaction path in which the dissociation of O-O bond proceeds after the O_2 adsorption state (b). However, it would be occasionally possible that one of the Si-O bonds is dissociated after structure (b) while maintaining the O-O bond. For example, the bond dissociation from the Si adatom would enable the O_2 molecule to rotate over the Si restatom and make another Si-O bond with an adjacent Si adatom, which would result in the hopping of bright sites in STM observations.

V. SUMMARY

Theoretical calculations suggested reaction paths of the O_2 molecules on Si(111) 7×7 surfaces. The reaction processes of an O_2 attack on the clean Si surface and another O_2 attack on the O_2 -adsorbed surface were closely examined with the cluster method. In both processes, stable molecular precursors appeared preceding the dissociative oxidized species, and the activation energies required for the O_2 dissociation for both processes were estimated to be 1.3 eV. The first O_2 adsorption on the Si surface generated a molecular stable state with an Si-O-O-Si formation, which was demonstrated to be imaged brightly in STM observations. A disso-

ciative stable state with an Si-O-Si-O formation and additional O₂-reacted states were suggested to be imaged darkly. Band calculations with the supercell method gave support to these conclusions, in which DOS curves for these stable states showed a compatibility with the UPS and STS data. Furthermore, the calculated electron distributions, charge transfers, and dipole moments were suggested to be consistent with many other experimental findings.

ACKNOWLEDGMENTS

A part of this work was performed with the assistance of ASET in MITI's R&D Program supported by NEDO. One of the authors (T.H.) was supported by a grant from the Futaba Electronics Memorial Foundation. The computer programs used were GAUSSIAN94 by Gaussian, Inc. and PLANE_WAVE by Molecular Simulations, Inc.

- ¹U. Höfer, P. Morgen, W. Wurth, and E. Umbach, Phys. Rev. B **40**, 1130 (1989); U. Höfer, A. Puschmann, D. Coulman, and E. Umbach, Surf. Sci. **211/212**, 948 (1989)
- ²G. Hollinger, J.F. Morar, F.J. Himpsel, G. Hughes, and J.L. Jordan, Surf. Sci. **168**, 609 (1986)
- ³C. Silvestre and M. Shayegan, Phys. Rev. B **37**, 10 432 (1988); C. Silvestre, J. Hladky, and M. Shayegan, J. Vac. Sci. Technol. A **8**, 2743 (1990).
- ⁴G. Dujardin, G. Comtet, L. Hellner, T. Hirayama, M. Rose, L. Philippe, and M.J. Besnard-Ramage, Phys. Rev. Lett. **73**, 1727 (1994).
- ⁵P. Bratu, K.L. Kompa, and U. Höfer, Phys. Rev. B **49**, 14 070 (1994).
- ⁶T. Hoshino, M. Tsuda, S. Oikawa, and I. Ohdomari, Surf. Sci. Lett. **291**, L763 (1993).
- ⁷T. Hoshino, M. Tsuda, S. Oikawa, and I. Ohdomari, Phys. Rev. B **50**, 14 999 (1994).
- ⁸K. Kato, T. Uda, and K. Terakura, Phys. Rev. Lett. **80**, 2000 (1998).
- ⁹T. Hoshino, Phys. Rev. B **59**, 2332 (1999).
- ¹⁰M.P. D'Evelyn, M.M. Nelson, and T. Engel, Surf. Sci. **186**, 75 (1987); J.R. Engstrom and T. Engel, Phys. Rev. B **41**, 1038 (1990).
- ¹¹M.L. Yu and B.N. Eldridge, Phys. Rev. Lett. **58**, 1691 (1987).
- ¹²K. Ohkubo, Y. Igari, S. Tomada, and I. Kusunoki, Surf. Sci. **260**, 44 (1992).
- ¹³J.R. Engstrom, D.J. Bonser, and T. Engel, Surf. Sci. **268**, 238 (1992).
- ¹⁴K. Tsukui, K. Endo, R. Hasunuma, O. Hirabayashi, N. Yagi, H. Aihara, T. Osaka, and I. Ohdomari, Surf. Sci. **328**, L553 (1995), and references therein.
- ¹⁵F.M. Leibsle, A. Samsavar, and T.C. Chiang, Phys. Rev. B **38**, 5780 (1988).
- ¹⁶Ph. Avouris, I.W. Lyo, and F. Bozso, J. Vac. Sci. Technol. B **9**, 424 (1991); Ph. Avouris and I.W. Lyo, Appl. Surf. Sci. **60/61**, 426 (1992).
- ¹⁷T. Hasegawa, M. Kohno, S. Hosaka, and S. Hosoki, Surf. Sci. **312**, L753 (1994).
- ¹⁸Ph. Avouris, and I.W. Lyo, Surf. Sci. **242**, 1 (1991).
- ¹⁹G. Dujardin, A. Mayne, G. Comtet, L. Hellner, M. Jamet, E. Le Goff, and P. Millet, Phys. Rev. Lett. **76**, 3782 (1996).
- ²⁰B. Schubert, Ph. Avouris, and R. Hoffmann, J. Chem. Phys. **98**, 7593 (1993); **98**, 7606 (1993).
- ²¹See, for example, A. Szabo and N. S. Ostlund, *Modern Quantum Chemistry* (MacMillan, London, 1982).
- ²²M.S. Gordon, J.S. Binkley, J.A. Pople, W.J. Pietro, and W.J. Hehre, J. Am. Chem. Soc. **104**, 2791 (1982).
- ²³S.H. Vosko, L. Wilk, and M. Nusair, Can. J. Phys. **58**, 1200 (1980).
- ²⁴N. Troullier and J.L. Martins, Solid State Commun. **74**, 613 (1990).
- ²⁵T. Watanabe, T. Hoshino, and I. Ohdomari, Surf. Sci. **389**, 375 (1997), and references therein.
- ²⁶K. Kumamoto, T. Hoshino, K. Kokubun, T. Ishimaru, and I. Ohdomari, Phys. Rev. B **52**, 10 784 (1995).
- ²⁷T. Hoshino, K. Kokubun, K. Kumamoto, T. Ishimaru, and I. Ohdomari, Jpn. J. Appl. Phys., Part 1 **34**, 3346 (1995).
- ²⁸T. Hoshino, S. Oikawa, M. Tsuda, and I. Ohdomari, Phys. Rev. B **44**, 11 248 (1991).
- ²⁹T. Hoshino, M. Hata, S. Oikawa, M. Tsuda, and I. Ohdomari, Phys. Rev. B **54**, 11 331 (1996).
- ³⁰G. Comtet, G. Dujardin, L. Hellner, T. Hirayama, M. Rose, L. Philippe, and M.J. Besnard-Ramage, Surf. Sci. **331-333**, 370 (1995).
- ³¹R. Martel, Ph. Avouris, and I.W. Lyo, Science **272**, 385 (1996).
- ³²K. Edamoto, Y. Kubota, H. Kobayashi, M. Onchi, and M. Nishijima, J. Chem. Phys. **83**, 428 (1985).
- ³³I.S. Hwang, R.L. Lo, and T.T. Tsong, Phys. Rev. Lett. **78**, 4797 (1997).